Simulations of modal active control applied to the self-sustained oscillations of the clarinet

SIMULATIONS OF MODAL ACTIVE CONTROL APPLIED TO THE SELF-SUSTAINED OSCILLATIONS OF THE CLARINET

Thibaut Meurisse, Adrien Mamou-Mani, Rene Causse
IRCAM - 1 Place Igor Stravinsky, 75004 Paris, France
Thibaut.Meurisse@ircam.fr

David Sharp
The Open University - Walton Hall, Milton Keynes, MK7 6AA, UK
David.Sharp@open.ac.uk

ABSTRACT

Modal active control enables modifications of the damping and the frequencies of the different resonances of a system. A self-sustained oscillating wind instrument is modelled as a disturbance coupled to a resonator through a non-linear coupling. The aim of this study is to present simulations of modal active control applied to a modeled simplified self-sustained oscillating wind instrument (e.g. a cylindrical tube coupled to a reed, which is considered to approximate a simplified clarinet), incorporating collocated speaker, microphone and a reed. The next goal will be to apply this control experimentally and to test it with musicians.

1. INTRODUCTION

Modal active control enables modifications of the damping and the frequencies of the resonances of a system [1, 2]. However, there have been relatively few applications for musical instruments [3–5] and no application to wind instruments to the authors' knowledge.

Self-sustained oscillating wind instruments, like the clarinet, are modeled as a disturbance coupled to a resonator through a non-linear coupling [6–9] (see Figure 1). By applying modal active control to a self-sustained simplified clarinet (e.g. a cylindrical tube coupled to a reed), it should be possible to modify its emitted sound and playability.

The aim of this study is to present simulations of modal active control applied to a simplified clarinet.

After presenting the clarinet model and the principles of the modal active control, a coupling between them is proposed. Then, simulations are presented of the control of the frequency and the damping of the first resonance, the control of the damping of the second resonance of a cylindrical tube and finally maps showing the control limits of the first resonance in frequency and damping.

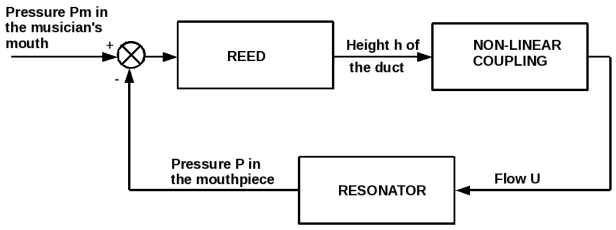

Figure 1. Model of a self-sustained wind instrument [6, 11].

2. MODELING

2.1 Self-Sustained Wind Instrument Model

Models of self-sustained wind instruments like the clarinet have been reported for over 30 years [6–10]. Classically, a self-sustained wind instrument can be described in terms of both linear (reed, resonator) and non-linear (coupling) elements (see Figure 1). In particular, the model used in this paper is the one described by [11].

In a clarinet, a single reed controls the flow of air from the player's mouth into the instrument. Let $h(t)$ be the position of the reed. Then,

$$\frac{1}{\omega_r^2}\frac{d^2h(t)}{dt^2} + \frac{q_r}{\omega_r}\frac{dh(t)}{dt} + h(t) - h_0 = -\frac{1}{K_r}(P_m - P(t)) \quad (1)$$

where ω_r is the resonance frequency of the reed, q_r its damping, h_0 its equilibrium position and K_r its stiffness, P_m is the pressure in the player's mouth, assumed to be constant, and $P(t)$ the pressure in the mouthpiece.

The pressure in the mouthpiece is obtained through the poles s_n and the residus C_n of the input impedance of the resonator. Let P_n be the pressure of the mode n. Then,

$$\frac{dP_n(t)}{dt} = s_n P_n(t) + Z_c C_n U(t) \quad (2)$$

where $Z_c = \rho_0 c/S$ is the characteristic impedance of the tube with S its cross-sectional area, ρ_0 the density of the

acoustic medium, c the velocity of sound in the medium and $U(t)$ the flow through the reed duct. The pressure is then

$$P(t) = 2\sum_n \Re(P_n) \tag{3}$$

Using the same hypothesis as described in [11], the flow can be determined from

$$U(t) = sign(P_m - P(t))Wh(t)\sqrt{\frac{2|P_m - P(t)|}{\rho_0}} \tag{4}$$

where W is the width of the reed duct.

2.2 Modal Active Control

Modal active control makes it possible to control the damping and the frequency of the eigenmodes of a system. To apply this control, it is necessary to build a model of the system. A state-space model of the system is implemented.

2.2.1 State-Space Model

The state-space model of the acoustic duct used in this paper is inspired by [1] and adapted to the simulation needs, using [2, 5, 12, 13]. The diameter $2R$ of the duct is sufficiently small compared to its length L_t, that the duct can be considered to be a one-dimensional waveguide with spatial coordinate z, where $0 \leq z \leq L_t$. The control speaker is placed at $z = z_s$. The microphone is placed at the same location ($z_m = z_s$).
The pressure in the duct is described by:

$$\frac{1}{c^2}\frac{\partial^2 p(z,t)}{\partial t^2} = \frac{\partial^2 p(z,t)}{\partial x^2} + \rho_0 \frac{dv_s(t)}{dt}\delta(z - z_s) \tag{5}$$

where p is the acoustic pressure and v_s the speaker baffle velocity.
Using separation of variables, let

$$p(z,t) = q(t)V(z) \tag{6}$$

where ([1, 14])

$$V_i(z) = c\sqrt{\frac{2}{L_t}}cos(k_i z) \tag{7}$$

where $V_i(z)$ is the amplitude of the mode i at position z and $k_i = (2i+1)\pi/2L_t$. To obtain a state-space description of the acoustic duct, without considering the mode of the speaker, let

$$x(t) = \begin{bmatrix} q \\ \dot{q} \end{bmatrix} \tag{8}$$

where $x(t)$ is the state vector so that

$$\dot{x}(t) = Ax(t) + Bu_s(t) + G\omega(t) \tag{9}$$

$$y(t) = Cx(t) \tag{10}$$

where

$$u_s = \rho_0 \dot{v_s} \tag{11}$$

is the command and $\omega(t)$ a disturbance signal at $z_d = 0$,

$$A = \begin{bmatrix} 0_{r,r} & I_{r,r} \\ -diag(\omega_i^2) & -diag(2\xi_i\omega_i) \end{bmatrix} \tag{12}$$

is the *system matrix* [15], I is the identity matrix, ξ_i is the damping of mode i and ω_i its frequency,

$$B = \begin{bmatrix} 0_{r,1} \\ V_i(z_s) \end{bmatrix} \tag{13}$$

is the *actuator matrix*,

$$C = \begin{bmatrix} V_i(z_m) & 0_{1,r} \end{bmatrix} \tag{14}$$

is the *sensor matrix*, and

$$G = \begin{bmatrix} 0_{1,r} \\ V_i(z_d) \end{bmatrix} \tag{15}$$

is the *disturbance matrix*.

2.2.2 Control of the Eigenmodes

The control is carried out using pole placement. The coordinates of the poles are defined by the damping and the angular frequency of each mode [2, 12]:

$$Re(pole_i) = \xi_i\omega_i \tag{16}$$

and

$$Im(pole_i) = \pm\omega_i\sqrt{1-\xi_i^2} \tag{17}$$

where ξ_i and ω_i are the damping and the angular frequency of the i^{th} mode.
It is then possible to dictate the damping and the frequency of each mode. Practically, the observer generates a control gain vector K and an observation gain vector L. The control gain vector K is chosen such that

$$det[sI - (A - BK)] = 0 \tag{18}$$

where $s = j\omega$. In the simulations, K is obtained using the Matlab *place* function [16] with the target poles. The observation gain vector L is used in the observer control loop such that

$$L(y - \hat{y}) \to 0 \tag{19}$$

where $\hat{y}$ is the observer estimation of y (see figure 2). In the simulations, L is obtained using *place* function with poles which real parts are two times the value of the poles used to obtain K.
The simulations show transfer functions obtained in open loop (without control) and closed loop (with control). Open loop transfer function H_{OL} is [13]:

$$H_{OL} = C(sI - A)^{-1}G \tag{20}$$

Closed loop transfer function H_{CL} is :

$$H_{CL} = C(sI - (A - BK(sI - (A - BK - LC))^{-1}LC))^{-1}G \tag{21}$$

2.3 Active Control on the Self-Sustained Model

2.3.1 Dimensionless Equations

To make it easier to implement, the self-sustained model is made dimensionless. Let

$$\begin{array}{c} x_h(t) = h(t)/h_0 \\ y_h(t) = h'(t)/v_0 \\ p_n(t) = P_n(t)/P_M \\ p(t) = P(t)/P_M \\ u(t) = U(t)Z_c/P_M \end{array} \tag{22}$$

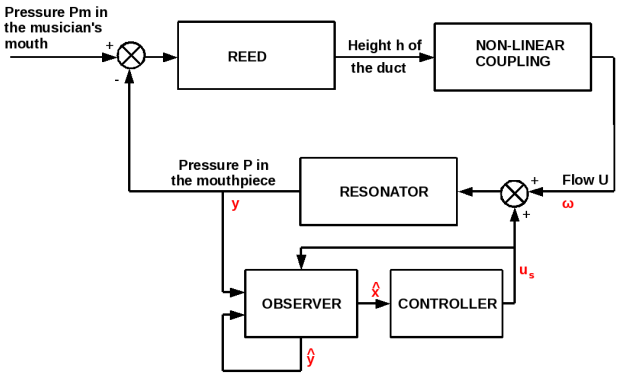

Figure 2. Model of a self-sustained wind instrument with control system. ω, y and u_s are defined in eq.(9) and (10). $\hat{y}$ and $\hat{x}$ are the observer estimations of y and x.

where $v_0 = h_0\omega_r$ is the reed's speed in free behaviour and $P_M = K_r h_0$ is the pressure required to completely close the reed channel in static regime. The final system is then

$$\begin{aligned} \tfrac{1}{\omega_r} x_h'(t) &= y_h(t) \\ \tfrac{1}{\omega_r} y_h'(t) &= 1 - x_h(t) + p(t) - \gamma - q_r y_h(t) \\ p_n'(t) &= C_n u(t) + s_n p_n(t) \\ p(t) &= 2\sum \Re(p_n(t)) \\ u(t) &= \zeta sign(\gamma - p(t)) x_h(t) \sqrt{|\gamma - p(t)|} \end{aligned} \tag{23}$$

where $\gamma = P_m/P_M$ represents the pressure in the musician's mouth, $\gamma \simeq 1/3 + \epsilon$ with $\epsilon \ll 1$ [8].
$\zeta = Z_c W \sqrt{\frac{2h_0}{\rho_0 P_M}}$ [9] represents the musician's lips on the mouthpiece.

2.3.2 Adaptating the Control

The design of the controller does not allow the control of the resonator described by the poles and residus. It is then necessary to adapt the state space implementation of the controller to the dimensionless self-sustained system. Eq.(23) shows that the input of the resonator is a flow u. Eq.(5) shows that the state-space resonator must have an acceleration as an input, the acceleration of the speaker baffle $\dot{v_s}$. From (11),

$$u_s = \rho_0 \frac{dv_s}{dt} = \frac{\rho_0}{S}\frac{dU}{dt} \tag{24}$$

where S is the cross-sectional area of the tube. To make the flow U dimensionless, it has been divided by the characteristic impedance of the tube Z_c between eq.(2) and eq.(23). Then,

$$u_s = \frac{\rho_0}{S Z_c}\frac{du}{dt} \tag{25}$$

In *Simulink*, the *discrete derivative* object is used to apply the differentiation.
It is then possible to couple the reed and the state-space resonator *via* the flow (see Figure 2).
Next section presents some results of the simulations.

3. SIMULATIONS

Simulations are carried out using *Matlab* and *Simulink*. The simulations are made with a closed-open tube with length $L_t = 1.09m$ and radius $R = 0.0109m$. The speaker and microphone are placed at the entrance of the tube ($z_s = z_m = 0$). The modal parameters (ξ_i, ω_i) of a calculated input impedance [17] are extracted thanks to a Rational Fraction Polynomials (RFP) algorithm [18]. The efficiency of the RFP algorithm has already been demonstrated [13, 19]. Only the 10 first resonances are modeled. The pole placement is obtained using the Matlab *place* function. Simulink is used in the *Fixed-step* mode, with the *ode3 (Bogacki-Shampine)* solver. The sample time is 1/44100, and the simulation time is 3s. The considered length is close to the length of a bass clarinet without bell and bocal, the modeled reed is then adapted to a bass clarinet reed. Table 1 shows the values that have been used in the simulation to characterise the reed. Figure 3 shows the shape of the dimensionless pressure input used.
Two cases are first presented. First, the frequency and the damping of the first resonance are controlled, and second, the damping of the second resonance is controlled. Effects of the control on the sound spectrum and the attack transient are studied. Then two maps are presented. The first shows the limits of the control of the frequency of the first resonance. The second shows the limits of the control of the damping of the first resonance.

f_r	1300Hz
q_r	1
K_r	3.3×10^8N/m
h_0	3×10^{-4}m
W	0.0168m

Table 1. Parameters used to characterise the bass clarinet reed.

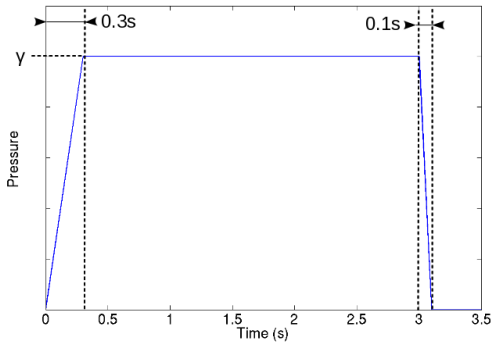

Figure 3. Shape of the dimensionless pressure input used for the simulations.

3.1 Control of the Frequency and the Damping of the First Resonance

The control is applied such that the frequency of the first resonance is changed, from 78Hz to 70Hz, and its damping is increased five times.

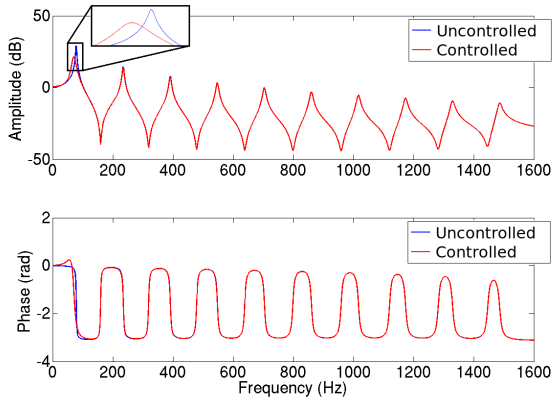

Figure 4. Top : Transfer functions of the uncontrolled (blue) and controlled (red) systems. The control aims to change the frequency of the first resonance from 78Hz to 70Hz and to increase its damping five times. Bottom : Phases of the transfer functions of the uncontrolled (blue) and controlled (red) resonators.

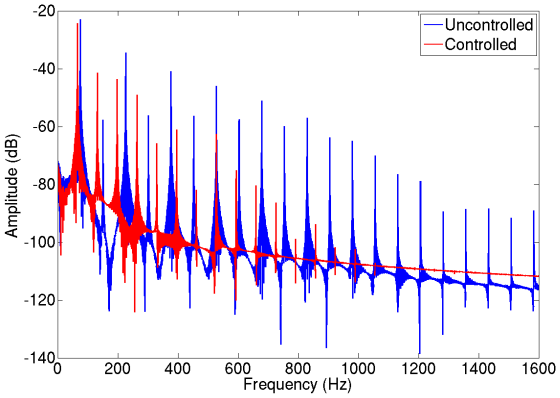

Figure 5. Sound spectra of the uncontrolled (blue) and controlled (red) self-sustained oscillating systems, with $\gamma = 0.3683$.

Figure 4 shows the transfer functions of the uncontrolled and controlled systems. With the control, the frequency of the first resonance is changed to 70.2Hz, and its amplitude is decreased by 7.7dB. The second resonance is also affected, with a decrease of 0.7dB.

Figure 5 shows the sound spectra of the steady states of the uncontrolled and controlled self-sustained systems, with $\gamma = 0.3683$. With the control applied, the simulation still plays on the first resonance of the instrument. Here, it is 66Hz, and 1.3dB lower than without control. As this resonance is no more tuned with the other resonances, there are fewer harmonics compared to the uncontrolled instrument, and no harmonics beyond 1000Hz. The last harmonic at 989Hz is 37dB lower than the closest harmonic of the uncontrolled instrument which is at 980Hz.

Figure 6 shows the attack transients of the uncontrolled and controlled self-sustained systems, with $\gamma = 0.3683$.

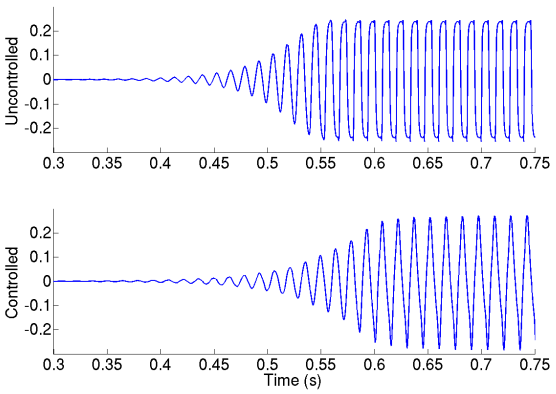

Figure 6. Attack transients of the uncontrolled (top) and controlled (bottom) self-sustained systems, with $\gamma = 0.3683$.

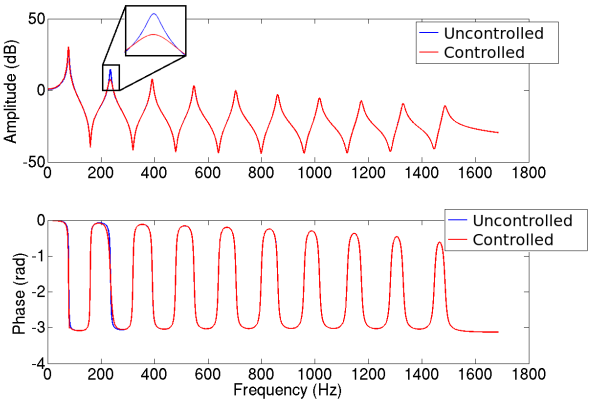

Figure 7. Top : Transfer functions of the uncontrolled (blue) and controlled (red) systems. The control aims to change the damping of the first resonance. It is increased 3 times. Bottom : Phases of the transfer functions of the uncontrolled (blue) and controlled (red) resonators.

Both cases are made blowing exactly in the same way in the tube. The transient is 0.06s longer in the controlled system, and the final amplitude is increased by 11%. The control changes the shape of the steady-state, from a square wave like signal to a sawtooth wave like signal.

3.2 Control of the Damping of the Second Resonance

The control is applied such that the damping of the second resonance is increased 3 times.

Figure 7 shows the transfer functions of the uncontrolled and controlled systems. With the control, the amplitude of the second resonance is decreased by 7dB. The first resonance is also affected by the control and is increased by 1.2dB.

Figure 8 shows the sound spectra of the steady states of the uncontrolled and controlled self-sustained systems, with $\gamma = 0.3533$. With the control applied, the number of harmonics in the sound decreases: seven harmonics when

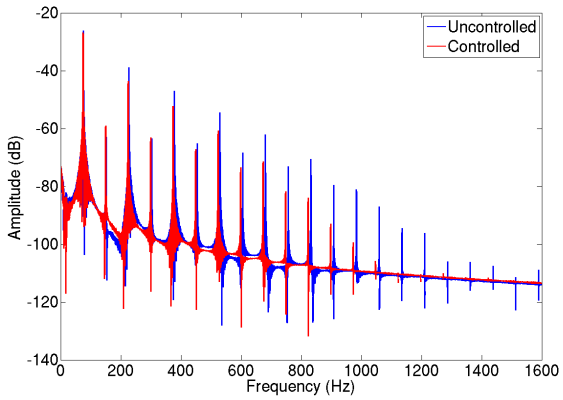

Figure 8. Sound spectra of the uncontrolled (blue) and controlled (red) self-sustained systems, with $\gamma = 0.3533$.

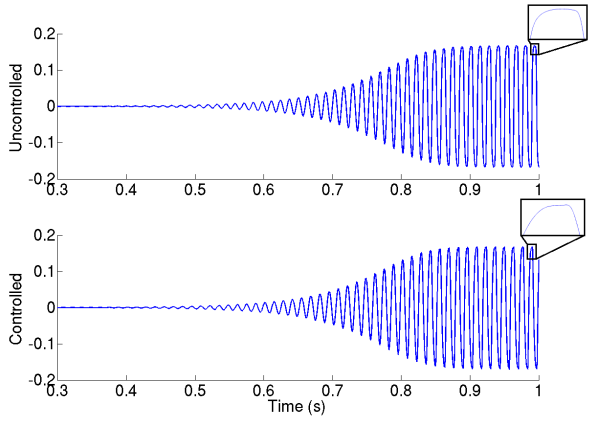

Figure 9. Attack transient of the uncontrolled (top) and controlled (bottom) self-sustained systems, with $\gamma = 0.3533$.

controlled, ten harmonics when uncontrolled. This comes with decreases of the amplitude of the resonances, from 0.6dB (first resonance) to 18.2dB (seventh resonance), and decreases of the frequency of the resonances, from 0.9Hz (first resonance) to 11.3Hz (seventh resonance).

Figure 9 shows the attack transients of the uncontrolled and controlled self-sustained systems, with $\gamma = 0.3533$. Both cases are made blowing exactly in the same way in the tube. The transients are longer than previously because the pressure in the musician's mouth is smaller. In the controlled system, the final shape of the signal is slightly different and its amplitude is increased by 1%.

3.3 Limits of the control of the frequency of the first resonance

The control is applied such that the frequency of the first resonance varies from 60Hz to 160Hz with a 1Hz step. For each frequency, γ varies from 0 (null pressure in the mouth of the musician) to 1 (the reed channel is closed in static regime) with a 0.002 step. Figure 10 shows which frequency is played (color) when the control moves the first resonance to these frequencies with these mouth pressures.

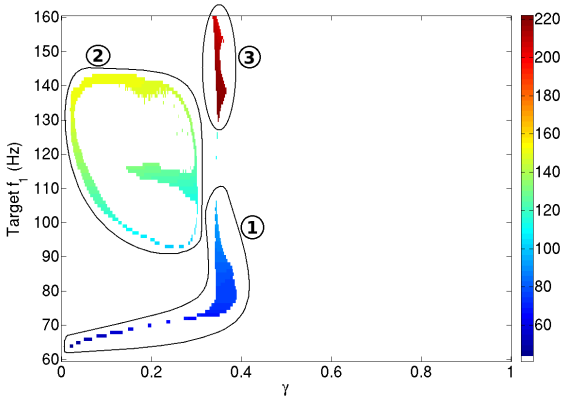

Figure 10. Map of the playing frequencies (color) regarding to the target frequency for the first resonance (ordinate) and to the pressure in the mouth of the musician (abscissa). White parts mean the model can not *play*.

In this section, to indicate a specific point, the $\{Target\ f_1; \gamma; Playing\ frequency\}$ formulation is chosen.

The map in figure 10 shows three parts (circled black).
In the first one, all the playing frequencies are lower than the frequency of the resonance. It gives the lowest playing frequencies, from $\{64; 0.018; 44\}$ to $\{106; 0.344; 100\}$. It also gives the highest mouth pressure with $\{78; 0.388; 75\}$, at the natural f_1 of the tube (78Hz). The playing frequencies have 45 cents ($\{78; 0.388; 75\}$) to 180 cents ($\{64; 0.018; 44\}$) differences with the frequency of the resonance.
In the second part, all the playing frequencies are higher than the frequency of the resonance. It shows stable solutions with low mouth pressures, between $\{133; 0.018; 149\}$ and $\{110; 0.302; 117\}$. The playing frequencies are between $\{93; 0.270; 100\}$ and $\{143; 0.068; 152\}$. The playing frequencies have 94 cents $\{143; 0.162; 151\}$ to 212 cents $\{115; 0.154; 130\}$ differences with the frequency of the resonance.
In the third part, all the playing frequencies are those of the second resonance, which is about 236Hz. As a consequence, this part shows the highest playing frequencies. The playing frequencies are between $\{130; 0.348; 222\}$ and $\{160; 0.344; 204\}$. It shows that the second resonance is influenced by the control of the first frequency, as its frequency also moves with large control. In this part, the stable solutions have a mouth pressure close to the main part of part 1, from $\{160; 0.336; 210\}$ to $\{138; 0.366; 217\}$.
There is no stable solution beyond $\gamma = 0.388$, whatever the control and with all the other parameters made constant. Globally, the frequency increases when the mouth pressure decreases. In these simulations, every target frequencies between 64Hz and 160Hz have at least one stable solution. The playing frequencies on the first resonance (parts 1 and 2) are between 44Hz and 152Hz, a 21 semitones interval (an octave is 12 semitones).

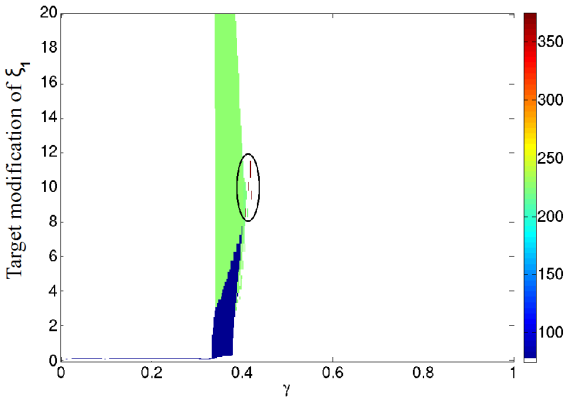

Figure 11. Map of the playing frequencies (color) regarding to the target modification of the damping of the first resonance (ordinate, $\xi = value \times \xi_1$) and to the pressure in the mouth of the musician (abscissa). White parts mean the model can not *play*.

3.4 Limits of the control of the damping of the first resonance

The control is applied such that the damping of the first resonance is :

- Decreased, from 0 to 1 times the natural damping (ξ_1) with a 0.05$\times$ step.
- Increased, from 1 to 5 times the natural damping with a 0.2$\times$ step.
- Increased, from 5 to 10 times the natural damping with a 0.5$\times$ step.
- Increased, from 10 to 20 times the natural damping with a 1$\times$ step.

For each damping, γ varies from 0 (null pressure in the mouth of the musician) to 1 (the reed channel is closed in static regime) with a 0.002 step. Figure 11 shows which frequency is played (color) when the control moves the first resonance to these dampings with these mouth pressures. In this section, to indicate a specific point, the $\{Target\ modification;\ \gamma;\ Playing\ frequency\}$ formulation is chosen.
The map in figure 11 shows three parts, the blue part, the green part and the red part (last is circled black).
In the first part, the playing frequency is the frequency of the first resonance. At low mouth pressures (from $\{0.1;\ 0.008;\ 78\}$ to $\{0.15;\ 0.344;\ 78\}$), the playing frequency is exactly the frequency of the first resonance. All the other stable solutions have mouth pressures close to $\gamma = 1/3$, with $0.344 < \gamma < 0.41$. With these mouth pressures, the playing frequencies varies from $\{7.5;\ 0.41;\ 75\}$ to $\{0.4;\ 0.344;\ 76\}$. The variations of the playing frequencies are almost null.
In the second part, the playing frequency is the frequency of the second resonance, when the damping of the first resonance is high enough. Between $\{3.2;\ 0.352;\ 227\}$ and $\{7.5;\ 0.414;\ 224\}$, the second and the first resonance are played alternatively when the mouth pressure is growing. Beyond, from $\{8;\ 0.352;\ 228\}$ to $\{20;\ 0.394;\ 226\}$, only the second resonance is played. The variations of the playing frequency is of about 3Hz.
Part 3 shows few stable solutions (four in figure 11) where the playing frequency is the frequency of the third resonance, which is about 393Hz. These solutions are at $\{8.5;\ 0.418;\ 375\}$, $\{9.5;\ 0.430;\ 373\}$, $\{10;\ 0.424;\ 374\}$ and $\{11;\ 0.428;\ 374\}$.
Most of the stable solutions have a mouth pressure such that $0.344 < \gamma < 0.414$. When the damping is high enough, the playing frequency becomes the second resonance. All the modifications of the damping between $0.1 \times \xi_1$ and $20 \times \xi_1$ have at least one stable solution.

4. CONCLUSION AND PERSPECTIVES

A complete model of a simplified controlled self-sustained oscillating wind instrument has been proposed in order to observe through the simulation of the effects of modal active control. Effects of this control on the sound spectrum and attack transient of a simplified clarinet have been observed. Maps of the control limits of the frequency and damping of the first resonance have been done. The control enables changes in damping and frequency of the resonances of the instrument.
An investigation of the limits of the simulation, that is finding the maximum changes in damping and frequency of the other resonances that are stable, has to be done. A stability study for the adaptation of the control to a real instrument is necessary. A study of the optimal position of the sensor (microphone) and actuator (speaker) regarding to a specific control will be done, then the application of the control to a real simplified instrument with the same dimensions will be done. Finally, playing and perceptive tests with musicians will be done.

Acknowledgments

This work was carried out during the PhD of Thibaut Meurisse, funded by Agence Nationale de la Recherche (ANR IMAREV project) and Universite Pierre et Marie Curie (UPMC, Paris). We thank gratefully Baptiste Chomette for his help with the RFP algorithm, and Sami Karkar and Fabrice Silva for their help with their clarinet model. We thank the Newton Fellowship for funding the collaboration between France and UK.

5. REFERENCES

[1] J. Hong et al, "Modeling, Identification, and Feedback Control of Noise in an Acoustic Duct," *IEEE Transactions on Control Systems Technology*, vol. 4, no. 3, May 1996.

[2] A.Preumont, *Vibration Control of Active Structures, An Introduction - Third Edition* Springer, 2011.

[3] E. Berdahl, J. Smith, "Feedback control of acoustic musical instruments: Collocated control using physical analogs", *J. Acoust. Soc. Am.*, vol. 131, pp.963-973, 2012.

[4] H. Boutin, *Methodes de controle actif d'instruments de musique. Cas de la lame de xylophone et du violon*. Phd Thesis, Universite Pierre et Marie Curie - Paris VI, 2011.

[5] S. Hanagud, S. Griffin, "Active Structural Control for a Smart Guitar," in *Proc. of the 4th European Conference On Smart Structures and Materials*, Harrogate, United Kingdom, July 6-8 1998.

[6] M. E. McIntyre, R. T. Schumacher, J. Woodhouse, "On the oscillations of musical instruments", *J. Acoust. Soc. Am.*, vol. 74, no. 5, pp.1325-1345, November 1983.

[7] R. T. Schumacher, "Self-Sustained Oscillations of the Clarinet: An Integral Equation Approach", *ACUSTICA*, vol. 40, pp.298-309, 1978.

[8] F. Silva, J. Kergomard, C. Vergez, J. Gilbert, "Interaction of reed and acoustic resonator in clarinetlike systems", *J. Acoust. Soc. Am.*, vol. 124, no. 5, pp.3284-3295, November 2008.

[9] S. Karkar, C. Vergez, B. Cochelin, "Oscillation threshold of a clarinet model: A numerical continuation approach", *J. Acoust. Soc. Am.*, vol. 131, no. 1, pp.698-707, January 2012.

[10] F. Silva, *Emergence des auto-oscillations dans un instrument de musique a anche simple*. Phd Thesis, Universite de Provence - Aix-Marseille I, 2009.

[11] S. Karkar, *Methodes numeriques pour les systemes dynamiques non lineaires - Application aux instruments de musique auto-oscillants*. Phd Thesis, Universite de Provence - Aix-Marseille I, 2012.

[12] K. Ogata, *Modern Control Engineering - Fourth Edition* Prentice Hall, 2002.

[13] B. Chomette, *Controles modaux actif, semi-adaptatif et semi-actif de structures intelligentes embarquees, Application aux cartes electroniques*. Phd Thesis, Institut National des Sciences Appliquees de Lyon, 2008.

[14] T. Meurisse, A. Mamou-Mani, R. Causse, D. Sharp, "Active control applied to wind instruments." in *Acoustics 2012*, Nantes, France, 23-27 April 2012.

[15] PA. Nelson, SJ. Elliot, *Active Control of Sound* Academic Press, 1992.

[16] J. Kautsky, N.K. Nichols, "Robust Pole Assignment in Linear State Feedback", *Int. J. Control*, vol. 41, pp.1129-1155, 1985.

[17] J. Kergomard, A. Chaigne, *Acoustique des instruments de musique* Belin, 2008.

[18] T. Richardson, D. Formenti, "Parameter estimation from frequency response measurements using rational fraction polynomials" in *1eIMAC Conference*, 1982.

[19] T. Meurisse, A. Mamou-Mani, R. Causse, D. Sharp, "Active control applied to simplified wind musical instrument", in *Proc. Int. Cong. on Acoustics 2013*, Montreal, Canada, 2-7 June 2013.